

Design, ADMET, PASS Prediction and Molecular Docking Studies of Novel pyrazolo[3,4-d]pyrimidines for Prospective of Anti-Cancer Agents

Sathish Kumar Mittapalli^{1*}; PhD , Jay Prakash Soni^{1*}; PhD , Parameshwar Ravula¹; PhD , Nimisha Jain¹; PhD , Amit Upadhyay¹; PhD 

¹Department of Pharmaceutical Chemistry, Amity Institute of Pharmacy, Amity University, Gwalior, Madhya Pradesh, India.

Abstract

The increased burden of cancer disease globally arouses the urgent need for the development of novel chemical agent with improved efficacy and potency which can provide selective therapeutic outcome to an individual cancer patient. In this connection the in-silico designing of novel scaffolds are greatly helpful evading the need for synthesizing and evaluating the series of large number compounds. We have constructed novel pyrazolopyrimidines with reference to existing fused pyrimidine standards like central aromatic heterocycles, spacers, hydrophobic heads and tails. We examined for the nature and biochemical targets, ADMET evaluations using various online tools and molecular docking analysis through Schrodinger suite studied binding affinities with reference to standards as well as co-crystals. We designed pyrazolopyrimidines 7a-j and 12a-j along with molecular docking studies revealed that few were potential candidates compared to standard scores against various target kinases. The hydroxyl moiety in 7b & 7d, hydroxyl in 7e with 4-bromo showed more bonding affinity towards targets and remaining compounds produced mild to moderate affinities against various targets. GLU339, GLU51, LEU83, SER345, ASP404, ASN391, and ASP348 are major residues for H-bonding interactions, PHE80, LEU83, GLN275 influenced hydrophobic bonding and ASP404 for nitro group, GLU339 for hydroxyl group, LYS89 for methoxy groups are key residues in binding affinity. We also identified the key residues of target proteins involved in the interaction with ligands at the active pocket. We believe that these results could benefit the future development of anticancer scaffold containing pyrazolopyrimidine motifs in the core structure.

Keywords: Cytotoxic, Drug-Likeness, Glide Score, Molinspiration, Pyrazolopyrimidine, Tyrosine Kinase.

Please cite this article as: Mittapalli SK, Soni JP, Ravula P, Jain N, Upadhyay A. Design, ADMET, PASS Prediction and Molecular Docking Study of Novel pyrazolo[3,4-d]pyrimidines for the Prospective of Anti-Cancer Agents. Trends in Pharmaceutical Sciences. 2023;9(2):147-158. doi: 10.30476/TIPS.2023.98639.1192

1. Introduction

One of the illnesses related to people's health burden in the modern era is cancer, brought on by mutation of various genes that control cell activity in response to particular environmental factors. The WHO states that cancer is the second largest cause of death worldwide with 7.4 million deaths in 2004 and an expected to increase 11.4 million deaths in 2030 (1). Although there has

been a significant advancement in the treatment of cancer, critical issues like adverse effects and drug resistance remain serious problems. Thus, the hunt for secure efficient chemotherapeutic drugs still in high demand. It has become apparent that various cellular/molecular processes involved in maintaining the cells, and causing the cell death to renew the old and dysfunctional cells. Such processes include apoptosis, ferroptosis, and necroptosis. Apoptosis (programmed cell death), and tumour suppressor genes (play an important role in repairing of damaged DNA) are crucial for cancer treat-

Corresponding Author: Sathish Kumar Mittapalli & Jay Prakash Soni, Department of Pharmaceutical Chemistry, Amity Institute of Pharmacy, Amity University, Gwalior, Madhya Pradesh, India
Email: sattisuma@gmail.com & jpsoni@gwa.amity.edu

ment. Likely, the elevated levels of ROS, including super oxides, peroxides and hydroxyl radicals have been linked to cancer cell death, apoptosis and lead to permanent cell damage (2). Hence, some possible approach to develop novel drugs for cancer may be restoration of the normal apoptotic pathways, and inhibition of enzymes involved in the growth of cancer cell (3). Among such enzymes, many of the human genome encoded protein kinases are involved in the development and progression of human cancer.

It is widely known that receptor tyrosine kinases (RTKs) are important regulators of cellular functions. RTKs inhibitors stop the phosphorylation of intracellular targets, which are frequently involved in cell growth or angiogenesis. The epidermal growth factor receptor (EGFR), which has undergone extensive research, is frequently regarded as the "prototypical" RTK, and known as oncogenic driver in many cancers. The discoidin domain receptors (DDR) are non-integrin collagen receptors that are members of the RTKs family, essential for controlling cellular functions (4-6). Inhibitors of these receptors are successful examples of targeted cancer therapies to date which include antibody therapeutics and small-molecule tyrosine kinase inhibitors.

The over-expression of PIM (Proviral Integration site for Moloney Murine Leukaemia Virus) kinases may lead to, (a) reduced apoptosis, (b) increased cell proliferation, (c) genomic instability; thus, they can involve in the development of cancer when over expressed. The inhibitor of PIM Kinases is the latest advances of anti-cancer research area (7). Cyclin-Dependent Kinase-2 (CDK-2) involves in a range of biological processes

alongside their pivotal role in cell cycle regulation; thus, becomes promising option to develop anticancer agents. CDK-2 controls S-phase and M-phases of the cell division; therefore, over expression may lead to abnormal cell-cycles directly related to cancer cell hyperproliferation. Hence, CDK-2 is regarded as a potentially therapeutic target for cancer therapy (8). In the last decade, numerous pyrazole analogues have been reported for wide range of bioactivities including anticancer (9-15). Pyrazolopyrimidine is a bioisostere of purine and received great attention in the designing anticancer scaffolds (16-17).

Previously reported kinase inhibitors such as PKI-166, erlotinib, gefitinib, lapatinib contain standard pharmacophoric moieties such as 2-amino-4-(pyridine-3-yl)pyrimidine scaffold with aliphilic piperazinyl benzamide (18-22). Likely, folic acid analogues, anticancer antimetabolites methotrexate, pemetrexed, and pralatrexate contain pyrazino-pyrimidine as their integral core (23-25). The previous reports on various compounds bearing pyrazole or its bioisosters suggest that pyrazolo-pyrimidines are superior in terms of their cytotoxicity (IC_{50}) potential compare to other derivatives. Abdellatif *et al.* reported that pyrazolo(3,4-d)pyrimidines-4-one scaffold, in which at position N-3 derivatised with the imino linker and the carbon with substituted phenyl ring analogues were effective against human breast adenocarcinoma cell line, MCF-7, with the IC_{50} value of 12 μ M. The benzylideneamino group on the antitumor activity was in the order $NO_2 > F > Cl > OCH_3 > H$ and azomethine spacer groups were more potent than the 5-(4-substituted phenyl) derivatives (Figure 1) (26-28).

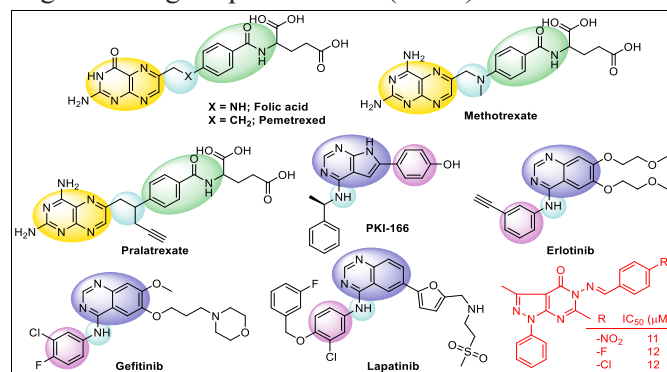
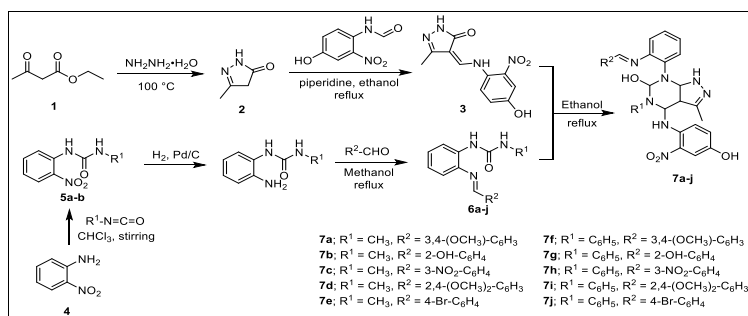


Figure 1. Structural features of antimetabolites, EGFR-RTKs inhibitors.



Scheme 1. Synthesis of novel 4, 6-dihydro-1H-pyrazolo[3,4-d]pyrimidines (7a-7j).

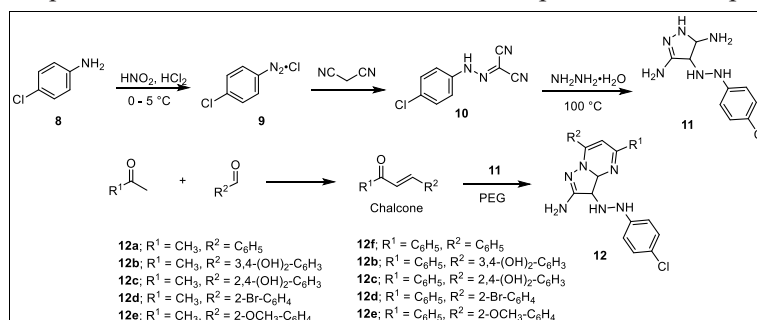
We have concentrated our efforts on identifying the pyrazolopyrimidine derivatives with anticancer action due to their intriguing biological properties. Herein, we have attempted the designing of bioisosteric analogues, containing pyrazolopyrimidine nucleus, linked with other lipophilic and hydrophilic groups. The primary aim of this research was to identify the novel pyrazolo[3,4-d]pyrimidines based on previously reported work with a rationale for anticancer drug discovery (29, 30).

We designed our molecular library by structural modifications of anilino-quinazolines via bioisosteric concepts. The modifications comprise replacement of quinazoline's benzene with pyrazole moiety expecting for the cytotoxic property. We performed various in-silico studies such as predicting physicochemical drug-likeness property, identification of potential biochemical targets, as well as molecular affinity and interaction with identified targets to evaluate these designed molecules as potential cytotoxic candidate. The rationale of designing the target compounds based on the structural modifications of general features of anilino-quinazolin compounds given in Figure 1. The possible modification comprises the replacing the benzene in the quinazoline nucleus with the

pyrazole moiety is found naturally in purine base pairs and this has been expected for the property of cytotoxicity. In response to these assertions, we describe a novel class of anticancer drugs based on 5, 6-disubstituted pyrazolo[3,4-d]pyrimidin-4-ones. Our strategy is to design a variety of compounds with diverse chemical properties, with the hope that the potency of these compounds can be increased by adding alternative binding groups to the pyrazolo[3,4-d]pyrimidine ring, such as a methyl group at position 6 and aroylhydrazone, phenylamino, amide, thioamide, thiosemicarbazide, and substituted aryl at position 5. These designed molecules can be easily accessed through the synthetic scheme illustrated in Scheme 1 and Scheme 2. The pyrazolopyrimidines scaffold may be constructed using one of two primary methods, the first of which begins with the pyrazole moiety and the second one begins with the pyrimidine moiety (31).

2. Materials and methods

ChemOffice 2020 (ChemDraw v20.1 and Chem3D v20.1) was used for drawing the chemical structures, as well as converting and viewing their 3D structure. Online tool SwissADME was used to predict all the physicochemical param-



Scheme 2. Synthesis of novel dihydropyrazolo[1,5-a]pyrimidin-7-yl]benzene-1,3-diols (12a-12j).

eters. The most probable protein/enzyme/receptor targets were predicted through SwissTargetPrediction online server and Molinspiration (Cheminformatics), a web server was used to generate the bioactivity scores. The protein crystal structures (PDB ID: 7ZUN, 2SRC & 7QHL) were obtained from Research Collaboratory for Structural Bioinformatics– Protein Data Bank (RCSB-PDB). Molecular docking analysis was performed using Glide module of Schrodinger suite v 2020-3. Computational algorithms were applied in order to find the best therapeutic candidate and cut down on the number of experimental studies. Simplified Molecular Input Line Entry System (SMILES) format was used to produce the molecule's ADME profile and drug-likeness criteria.

3. Experimental

3.1. Finding Molecular Descriptors

SwissADME online tool was used to predict the drug-likeness properties, which is the initial stage of drug development process (32). The primary properties for drug candidate are molecular weight, absorption, minimal molecular flexibility (measured in terms of number of rotatable bonds), and minimal total polar surface area (measured in terms of TPSA) (33). Simple molecular data, such as "molecular weight, number of hydrogen bond acceptors and donors, and partition coefficient of a molecule" can be used to determine a compound's permeability and bioavailability (34). Christopher A. Lipinski (1997) provided a key guideline for evaluating medication similarity known as Lipinski's rule of five (RO5). RO5 criteria is used to determine if a chemical might be an orally active medicine in the human body based on its biological and pharmacological characteristic (35). According to this criterion, a molecule qualifies as a drug moiety if it meets the criteria as follows; (a) 5 hydrogen bond donors, (b) 10 hydrogen bond acceptors, (c) partition coefficients value, logP (O/W), should be equal or less than 5, and (d) molecular weight should not exceed 500 Daltons.

3.2. Calculation of Bioactivity Score

The web-based online "Molinspiration" server was used to score the proposed compounds

for its bioactivity, inhibitory potential against different receptor and enzymes (36). A chemical may have significant biological activity if its bioactivity score is greater than 0.00, moderate biological activity is predicted for scores between -0.50 and 0.00, and inactivity is predicted for scores below -0.50.

3.3. Molecular Docking Analysis

The crystal structure of PIM kinase, receptor tyrosine kinase and cyclin dependent kinase has been retrieved from Protein Data Bank (PDB ID: 7ZUN, 2SRC & 7QHL). The protein preparation tool in Schrodinger suite 20.3 was used to prepare protein structure. The missing atoms were added, peripheral water molecules were removed at a distance of less than 5 Å from the binding pocket, and the structure was energetically minimized through the protein preparation wizard. The grid was generated by picking the active site where the co-crystal locates with a grid box at the centre of bound co-crystal. The designed ligands were drawn using 2D sketcher and subjected to energy minimization, followed by ligand preparation for the generation of different conformers using the LigPrep module of the Schrodinger 20.3. The different conformers thus obtained were subjected to molecular docking with Glide in standard precision (SP) mode. The poses generated were evaluated and the best-ranked pose was described.

4. Results and Discussion

4.1. The Molecular Descriptors

The molecular fingerprint (FP), which consists of a series of bits describing the presence or absence of chemical characteristics in a molecule, is one of the most well-known instances. This section compiles straightforward molecular and physical characteristics such as molecular weight (MW), number of rotatable bonds (nrotb), number of hydrogen bond donor (HBD), number of hydrogen acceptor (HBA), molecular refractivity (MR), count of particular atom kinds, and total polar surface area (TPSA). Also found quantitative estimate of drug-likeness (As good as QED close to 1) and number of violations from the Lipinski's RO5. The results presented in Table 1 advocate that all the compounds were within the limitations

Table 1. Molecular descriptive properties of designed compounds predicted by SwissADME.

S. No.	Entry	Chemical formula	MW ^a	HBD ^b	HBA ^c	LogP ^d	QED ^e	TPSA ^f	nrotbg	RO5 ^h
1	7a	C28H29N7O6	559.58	5	12	4.2	0.35	161.61	8	2
2	7b	C26H25N7O5	520.53	5	11	3.9	0.31	163.38	6	3
3	7c	C26H24N8O6	544.52	4	12	4.3	0.21	186.29	7	2
4	7d	C26H25N7O6	531.53	5	10	3.2	0.69	183.61	8	2
5	7e	C26H24BrN7O4	578.43	5	10	4.9	0.16	143.15	6	1
6	7f	C33H31N7O6	621.65	4	13	2.7	0.07	161.61	5	1
7	7g	C31H27N7O5	577.60	5	12	2.8	0.07	163.38	6	1
8	7h	C31H26N8O6	606.59	4	14	1.8	0.1	161.61	5	1
9	7i	C33H31N7O6	621.65	4	13	2.6	0.07	161.61	7	2
10	7j	C31H26BrN7O4	640.49	4	11	3.1	0.73	143.15	6	1
11	12a	C22H23ClN6	406.92	4	6	4.2	0.65	78.04	5	0
12	12b	C24H21ClN6O2	460.93	6	8	3.5	0.28	118.5	6	0
13	12c	C19H19ClN6O2	398.85	6	8	2.7	0.5	118.5	5	0
14	12d	C19H18BrClN6	445.75	4	6	4.1	0.63	78.04	7	0
15	12e	C20H21ClN6O	396.88	4	7	3.6	0.68	87.27	5	0
16	12f	C27H25ClN6	468.99	4	6	4.8	0.62	78.04	5	0
17	12g	C24H21ClN6O2	460.93	6	8	3.5	0.29	118.5	7	0
18	12h	C24H21ClN6O2	460.93	6	8	3.5	0.37	118.5	6	0
19	12i	C24H20BrClN6	507.82	4	6	4.7	0.53	78.04	6	1
20	12j	C25H23ClN6O	458.95	4	7	4.5	0.48	87.27	7	0

^aMolecular weight (g/mol); ^bHydrogen bond donor; ^cHydrogen bond acceptor; ^dLipophilicity, Octanol: Water partition coefficient; ^eQuantitative estimate of drug-likeness (as good as near to 1); ^fTopological polar surface area in Å²; ^gNumber of rotatable bonds; ^hNumber of violation from the Lipinski's rule of five.

except few were exemptible parameters like mass and HBA (Table 1).

4.2. Bioactivity Scoring (PREDICTION)

All the designed compounds, 7a-7j and 12a-j were screened as GPCR ligands, ion channel modulator, kinase inhibitors, nuclear receptor ligands, protease inhibitors, and enzyme inhibitors. The molecules 7a-7j targeted cyclin-dependent kinases (CDKs 1, 2, and 5), serine/threonine-protein kinase (PIM2), tyrosine-protein kinase, estrogen-receptor alpha (ER α), vascular endothelial growth factor receptor 2 (VEGFR2), melanocortin receptors, phosphodiesterase. Similarly, compounds 12a-12j targeted cannabinoid receptors, serine/threonine-protein kinase (PLK1), caspase-6, CDK2, epidermal growth factor receptor (EGFR), DNA-topoisomerase I complex, and tyrosine-protein kinase (JAK-3). Most of these biochemical targets are playing crucial role in oncogenesis processes. Among the compounds 7a-7j and 12a-j

screened for different targets, it has been demonstrated that that 60% of them target kinases, primarily PIM1. These proto-oncogenes are serine/threonine kinase and are important in cell proliferation and survival, giving a selective advantage in carcinogenesis. These molecules exert their oncogenic activity by regulating MYC transcription (MYC phosphorylation increases the protein's stability, thus, increases transcriptional activity), control of cell cycle progression, and phosphorylation as well as inhibition of pro-apoptotic proteins like BAD, MAP3K5, FOXO3. Compound 7b targets CDK2, which is a serine/threonine protein kinase and controls the cell cycle. CDK2 participates in mitosis but not in meiosis. The compound 7c targets beta-secretase 2 (BACE2), responsible for the amyloid precursor protein's proteolytic processing (APP). Releases beta-cleaved soluble APP and a matching cell-associated C-terminal fragment that is later released by gamma-secretase after cleaving APP between residues 690 and 691. The predicted

Table 2. Bioactivity score of designed compounds by Molinspiration.

S. No.	Entry	GPCR ligand	Ion Channel modulator	Kinase inhibitor	Nuclear Receptor ligand	Protease inhibitor	Enzyme inhibitor
1	7a	-0.31	-0.37	-0.45	-0.56	-0.47	-0.15
2	7b	-0.38	-0.15	-0.48	-0.64	-0.45	-0.32
3	7c	-0.1	-0.25	-0.29	-0.57	-0.24	-0.25
4	7d	-0.36	-0.45	-0.15	-0.79	-0.58	-0.19
5	7e	-0.35	-0.37	-0.16	-0.18	-0.65	-0.54
6	7f	-0.32	-0.18	-0.54	-0.18	-0.41	-0.58
7	7g	-0.24	-0.28	-0.41	-0.74	-0.35	-0.18
8	7h	-0.19	-0.28	-0.47	-0.85	-0.44	-0.37
9	7i	-0.35	-0.40	-0.45	-0.81	-0.41	-0.3
10	7j	-0.39	-0.49	-0.52	-0.79	-0.45	-0.31
11	12a	-0.09	-0.10	-0.25	-0.52	-0.15	-0.02
12	12b	-0.14	-0.24	-0.35	-0.68	-0.32	-0.21
13	12c	-0.24	-0.31	-0.41	-0.69	-0.35	-0.22
14	12d	-0.27	-0.30	-0.42	-0.87	-0.38	-0.28
15	12e	-0.3	-0.39	-0.49	-0.85	-0.42	-0.32
16	12f	-0.1	-0.20	-0.26	-0.54	-0.15	-0.12
17	12g	-0.11	-0.28	-0.31	-0.64	-0.26	-0.19
18	12h	-0.19	-0.33	-0.35	-0.65	-0.29	-0.2
19	12i	-0.22	-0.33	-0.36	-0.79	-0.31	-0.25
20	12j	-0.25	-0.40	-0.42	-0.78	-0.34	-0.28

bioactivity result for all the compounds 7a-j and 12a-j is presented in Table 2.

4.3. Assessment of Binding Affinity with Selected Biological Targets

Furthermore, all the compounds were subjected to molecular docking with three selected biochemical targets playing vital role in cancer, namely PIM kinase 1 (PDB ID: 7ZUN), RTKs (PDB ID: 2SRC) and CDK2 (PDB ID: 7HQL). The serine/threonine-protein kinase PIM1 (7ZUN) is a single chain protein consist of 314 amino acid residues, with the co-crystal 3, 4-dihydropyrrolo[1,2-a]pyrazin-1-ol. The molecular docking of all the ligands 7a-j and 12a-j along with references drug candidates (doxorubicin, imatinib, methotrexate and pemetrexed), as well as co-crystal. The molecular docking results presented in Table 3 shows docking score of newly designed ligands in the range of -4.51 to -6.49 and glide emodel score in the range of -27.35 to -64.58. To illustrate, compounds 7e, 7g and 12h have docking score of -6.49, -6.41, -6.64; and glide emodel score of -56.48, -63.44, -64.58,

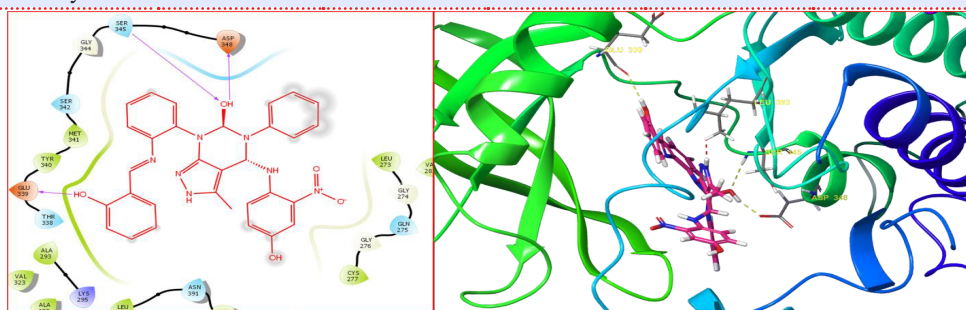
respectively. These results are well comparable with docking analysis of reference drugs (docking score = -4.16 to -7.47; glide emodel score = -41.08 to -97.89) and co-crystal (docking score = -7.87; glide emodel score = -69.24).

Similarly, tyrosine-protein kinase (2SRC) is also single peptide/protein chain consist of 452 amino acid residues with co-crystal structure namely phosphoramino phosphonic acid-adenylate ester. The docking score of newly designed ligands was found in the range of -4.897 to -9.052 and glide emodel score in the range of -45.255 to -96.537. For instances, compounds 7b, 7g and 7j have docking score of -8.66, -8.64, -9.05; and glide emodel score of -96.53, -65.83, -94.55, respectively. These results are well comparable with docking analysis of reference drugs (docking score=-5.82 to -8.81; glide emodel score =-63.38 to-95.06) and co-crystal (docking score =-9.75; glide emodel score =-139.14).

The next biochemical target selected was CDK2(PDB ID: 7QHL), which consist of two peptides chain with the total length of 209 amino acid

Table 3. Molecular Docking Simulations against potential Kinases (PIM Kinase, RTK and CDK2).

S. No.	Entry	7ZUN (PIM Kinase)		2SRC (Tyrosine kinase)		7QHL (CDK2)	
		Glide emodel	Docking score	Glide emodel	Docking score	Glide emodel	Docking score
1	7a	-56.52	-5.23	-83.30	-8.38	-81.81	-7.03
2	7b	-60.34	-6.05	-96.54	-8.66	-73.98	-8.10
3	7c	-61.76	-5.58	-89.65	-8.35	-63.29	-7.70
4	7d	-52.69	-5.70	-96.23	-8.42	-77.72	-7.94
5	7e	-56.48	-6.49	-73.81	-8.27	-82.93	-6.42
6	7f	-27.36	-5.86	-88.43	-7.75	-50.05	-6.60
7	7g	-63.44	-6.41	-65.84	-8.65	-35.85	-8.16
8	7h	-42.53	-5.99	-91.43	-8.50	-58.96	-6.43
9	7i	-36.83	-5.97	-54.68	-7.24	-59.43	-7.17
10	7j	-45.26	-6.01	-94.55	-9.05	-62.59	-7.14
11	12a	-47.47	-5.23	-54.01	-6.10	-55.81	-6.64
12	12b	-52.64	-4.89	-45.25	-4.90	-61.65	-6.80
13	12c	-54.55	-4.51	-66.02	-7.19	-61.08	-6.70
14	12d	-51.59	-5.03	-59.32	-5.97	-54.69	-6.00
15	12e	-46.07	-5.03	-53.52	-5.55	-52.02	-5.91
16	12f	-62.15	-5.61	-62.73	-6.53	-63.60	-6.43
17	12g	-61.78	-5.66	-59.32	-5.64	-62.46	-5.61
18	12h	-64.59	-6.44	-77.12	-7.04	-71.64	-6.91
19	12i	-53.45	-5.42	-63.97	-5.96	-61.41	-5.97
20	12j	-52.60	-5.23	-62.25	-6.30	-67.64	-6.49
21	Doxorubicin	-97.89	-7.47	-95.07	-8.81	-89.17	-8.92
22	Imatinib	50.24	-4.75	-63.39	-5.82	-77.60	-6.51
23	Methotrexate	-42.06	-4.16	-84.81	-7.65	74.75	-6.81
24	Pemetrexed	-41.08	-4.74	-84.83	-7.65	-88.37	-8.34
25	Co-Crystal	-69.24	-7.87	-139.14	-9.76	-99.35	-10.76

**Figure 2.** Structural features of antimetabolites, EGFR-RTKs inhibitors.

residues and with the co-crystal namely 5-(2-amino-1-ethyl)thio-3-cyclobutyl-7-[4-(pyrazol-1-yl)benzyl]amino-1(2H)-pyrazolo[4,3-d]pyrimidine. The docking score of our designed ligands was observed in the range of -5.67 to -8.15 and glide emodel score in the range of -35.84 to -82.93 . To demonstrate, compounds 7b, 7d and 7g have dock-

ing score of -8.10 , -7.95 , -8.16 ; and glide emodel score of -73.98 , -77.73 , -35.84 , respectively. These results are well comparable with docking analysis of reference drugs (docking score = -6.51 to -8.93 ; glide emodel score = -74.75 to -89.18) and co-crystal (docking score = -10.76 ; glide emodel score = -99.35).

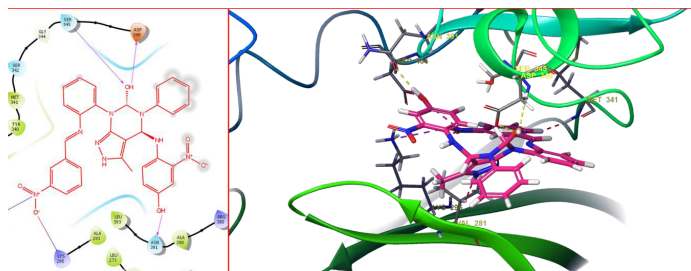


Figure 3. Binding interaction of compound 7h with RTKs (2SRC) in 2D and 3D mode; showing electrostatic interactions with SER345, ASP348, ASN391 and ASP404.

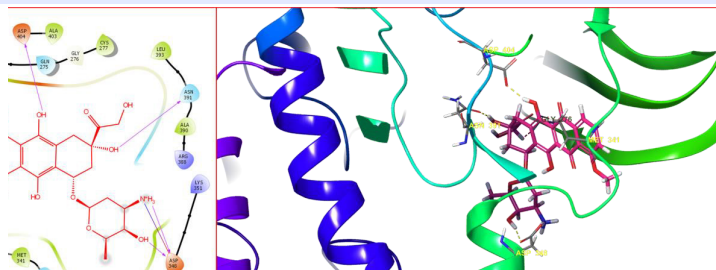


Figure 4. Binding interaction of reference drug doxorubicin with RTKs (2SRC) in 2D and 3D mode; showing electrostatic interactions with ASP348, ASN391 and ASP404.

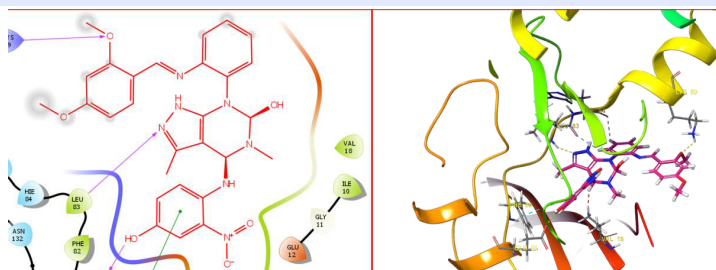


Figure 5. Binding interaction of compound 7d with CDK2 (7QHL) in 2D and 3D mode; having major electronic interactions with GLU51, PHE80, LEU83 and LYS89.

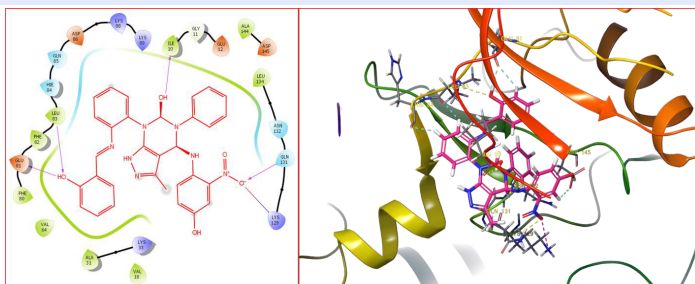


Figure 6. Binding interaction of compound 7g with CDK-2 (7QHL) in 2D and 3D mode; having major electronic interactions with ILE10, GLU81, LEU83, LYS129 and GLN131.

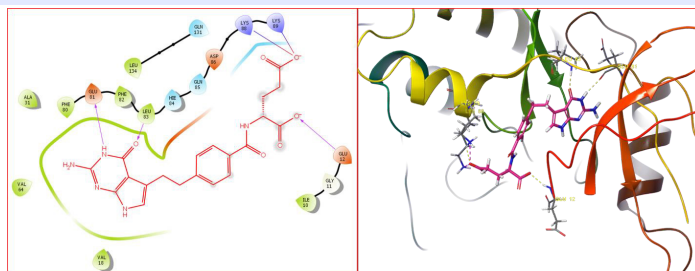


Figure 7. Binding interaction of reference drug pemetrexed with CDK-2 (7QHL) in 2D and 3D mode; having major electronic interactions with GLU12, GLU81, LEU83, LYS88 and LYS89.

In addition, some of the illustrative molecular interactions (2D interactions and 3D molecular pose) of most promising ligands are produced in Figure 2, Figure 3 and Figure 4 for tyrosine-protein kinase, 2SRC. Likewise, interaction diagrams for CDK2, 7QHL is presented in Figure 5, Figure 6 and Figure 7 showing interactions with different active site's residues.

5. Conclusion

The design of new kinase selective inhibitors and analysis of the compounds using ADMET filters and molecular docking studies may be used to summarize up the current investigation. Among all the 20 compound library, we found 10 compounds were less than or equal to one violation, 7a, 7d, 7j, 12f, and 12j with more than 0.5 QED, majority were screened as pim, tyrosine kinase, cyclin-dependent kinase 1/cyclin B1, p53-binding protein Mdm-2 biochemical targets.

Isoform of Serine/threonine-protein kinase pim-1 and co-crystal with docking score -7.867 K.Cal per mole, while 7g and 7h scores -6.853 and -6.421 compared to standard doxorubicin scored -7.494 K.Cal per mole, the biochemical target tyrosine-protein kinase SRC with co-crystal docking score -9.758 K.Cal per mole, while 7j and 7g scored -9.449 and -9.09 compared to standard doxorubicin scored -8.787 K. Cal per mole and finally the biochemical target cyclin-dependent kinase-2 and co-crystal with potential docking score -10.765, while 7d and 7e with the scores -9.119 and -8.63 compared with standard

References

1. Travis WD, Brambilla E, Nicholson AG, Yatabe Y, Austin JHM, Beasley MB, et al. The 2015 World Health Organization Classification of Lung Tumors: Impact of Genetic, Clinical and Radiologic Advances Since the 2004 Classification. *J Thorac Oncol.* 2015 Sep;10(9):1243-1260. doi: 10.1097/JTO.0000000000000630. PMID: 26291008.
2. Knaus UG. Oxidants in Physiological Processes. *Handb Exp Pharmacol.* 2021;264:27-47. doi: 10.1007/164_2020_380. PMID: 32767144.
3. Cordeu L, Cubedo E, Bandrés E, Rebollo A, Sáenz X, Chozas H, et al. Biological profile of new apoptotic agents based on 2,4-pyrido[2,3-

doxorubicin scored -8.897 K.Cal per mole. The substituent's 2,4 dimethoxy in 7d, 2-hydroxy in 7g and 4-bromo in 7j showed more bonding affinity towards targets and remaining compounds reported mild to moderate affinities against various targets (Figures 1-6). After summarization of all the results, it can be concluded that certain compounds have favourable bioactivity score, adequate drug likeness, drug score, and higher probability and they can possess anti-cancer activity. These compounds, specifically 4-[2-[6-hydroxy-4-(4-hydroxy-2-nitroanilino)-3,5-dimethyl-4,6-dihydro-1H-pyrazolo[3,4-d]pyrimidin-7-yl]phenyl]iminomethyl]benzene-1,3-diol (7d), 4-(4-hydroxy-2-nitroanilino)-7-[2-[(2-hydroxyphenyl)methylideneamino]phenyl]-3-methyl-5-phenyl-4,6-dihydro-1H-pyrazolo[3,4-d]pyrimidin-6-ol (7g), 7-[2-[(4-bromophenyl)methylideneamino]phenyl]-4-(4-hydroxy-2-nitroanilino)-3-methyl-5-phenyl-4,6-dihydro-1H-pyrazolo[3,4-d]pyrimidin-6-ol (7j) had better interactions with 2SRC and 7QHL. A few of the chosen compounds could be used as a reference point for the development of novel kinase inhibitors that are effective anticancer agents.

Acknowledgement

The authors would like to thank the management of Amity University, Madhya Pradesh for giving an opportunity to carry out this research.

Conflict of Interest

None declared.

- d]pyrimidine derivatives. *Bioorg Med Chem.* 2007 Feb 15;15(4):1659-69. doi: 10.1016/j.bmc.2006.12.010. Epub 2006 Dec 12. PMID: 17204425.
4. Yamaoka T, Kusumoto S, Ando K, Ohba M, Ohmori T. Receptor Tyrosine Kinase-Targeted Cancer Therapy. *Int J Mol Sci.* 2018 Nov 6;19(11):3491. doi: 10.3390/ijms19113491. PMID: 30404198; PMCID: PMC6274851.
5. Gan HK, Walker F, Burgess AW, Rigopoulos A, Scott AM, Johns TG. The epidermal growth factor receptor (EGFR) tyrosine kinase inhibitor AG1478 increases the formation of inactive untethered EGFR dimers. Implications for combination therapy with monoclonal antibody 806. *J Biol*

Chem. 2007 Feb 2;282(5):2840-50. doi: 10.1074/jbc.M605136200. Epub 2006 Nov 8. PMID: 17092939.

6. Kim G, Ko YT. Small molecule tyrosine kinase inhibitors in glioblastoma. *Arch Pharm Res.* 2020 Apr;43(4):385-394. doi: 10.1007/s12272-020-01232-3. Epub 2020 Apr 1. PMID: 32239429.
7. Tahvanainen J, Kyläniemi MK, Kanduri K, Gupta B, Lähteenmäki H, Kallonen T, et al. Proviral integration site for Moloney murine leukemia virus (PIM) kinases promote human T helper 1 cell differentiation. *J Biol Chem.* 2013 Feb 1;288(5):3048-58. doi: 10.1074/jbc.M112.361709. Epub 2012 Dec 3. PMID: 23209281; PMCID: PMC3561529.
8. Bettencourt-Dias M, Hildebrandt F, Pellman D, Woods G, Godinho SA. Centrosomes and cilia in human disease. *Trends Genet.* 2011 Aug;27(8):307-15. doi: 10.1016/j.tig.2011.05.004. Epub 2011 Jun 15. PMID: 21680046; PMCID: PMC3144269.
9. Akhramez S, Oumessaoud A, Hibot A, Talbi S, Hamri S, Ketatni EM, et al. Synthesis of pyrazolo-enaminones, bipyrazoles and pyrazolopyrimidines and evaluation of antioxidant and antimicrobial properties. *Arab J Chem.* 2022; 15(1):103527.
10. Shalai Y.R, Popovych M.V, Mandzynets S.M, Hreniukh V P, Finiuk N.S, Babsky A.M. Prooxidant and antioxidant processes in lymphoma cells under the action of pyrazolopyrimidine derivative. *Studia Biologica.* 2020;14(4):15-22.
11. Singh S, Gousuddin M. Synthesis of Pyrazolopyrimidine Derivatives and Its Antioxidants Activity. *Educ Psychol.* 2020;57(9):7272-86
12. Fekri A, Keshk EM, Khalil AM, Taha I. Synthesis of novel antioxidant and antitumor 5-aminopyrazole derivatives, 2D/3D QSAR, and molecular docking. *Mol Divers.* 2022 Apr;26(2):781-800. doi: 10.1007/s11030-021-10184-9. Epub 2021 Mar 8. PMID: 33683569.
13. Hassan A, El-Hifnawi H, Ahmed W. Design, Synthesis and in Vitro Evaluation of Antimicrobial and Anticancer Activity of Some Novel α,β -Unsaturated Ketones and their Corresponding Fused Pyridines. *J Adv Pharm Res.* 2019; 3(3): 117-133. doi: 10.21608/aprh.2019.10458.1081
14. El-Sayed R. Synthesis of an Efficiency Heterocyclic Systems, Surface Properties and Potential Pharmacological Interest. *J Oleo Sci.*

2018;67(8):991-1003. doi: 10.5650/jos.ess17222. PMID: 30068829.

15. Fahim AM, Farag AM, Shaaban MR, Rabag EA. Regioselective synthesis and DFT study of novel fused heterocyclic utilizing Thermal heating and Microwave Irradiation. *Afinidad.* 2018 Jun 30;75(582):148-159.
16. Gauthier A, Ho M. Role of sorafenib in the treatment of advanced hepatocellular carcinoma: An update. *Hepatol Res.* 2013 Feb;43(2):147-54. doi: 10.1111/j.1872-034X.2012.01113.x. Epub 2012 Nov 12. PMID: 23145926; PMCID: PMC3574194.
17. Nassar IF, Abdel Aal MT, El-Sayed WA, A E Shahin M, Elsakka EGE, Mokhtar MM, et al. Discovery of pyrazolo[3,4-d]pyrimidine and pyrazolo[4,3-e][1,2,4]triazolo[1,5-c]pyrimidine derivatives as novel CDK2 inhibitors: synthesis, biological and molecular modeling investigations. *RSC Adv.* 2022 May 17;12(23):14865-14882. doi: 10.1039/d2ra01968j. PMID: 35702208; PMCID: PMC9112407.
18. Traxler P, Bold G, Frei J, Lang M, Lydon N, Mett H, et al. Use of a pharmacophore model for the design of EGF-R tyrosine kinase inhibitors: 4-(phenylamino)pyrazolo[3,4-d]pyrimidines. *J Med Chem.* 1997 Oct 24;40(22):3601-16. doi: 10.1021/jm970124v. PMID: 9357527.
19. Smith J. Erlotinib: small-molecule targeted therapy in the treatment of non-small-cell lung cancer. *Clin Ther.* 2005 Oct;27(10):1513-34. doi: 10.1016/j.clinthera.2005.10.014. PMID: 16330289.
20. Druker BJ. Imatinib as a paradigm of targeted therapies. *Adv Cancer Res.* 2004;91:1-30. doi: 10.1016/S0065-230X(04)91001-9. PMID: 15327887.
21. Jin X, Mo Q, Zhang Y, Gao Y, Wu Y, Li J, et al. The p38 MAPK inhibitor BIRB796 enhances the antitumor effects of VX680 in cervical cancer. *Cancer Biol Ther.* 2016 May 3;17(5):566-76. doi: 10.1080/15384047.2016.1177676. PMID: 27082306; PMCID: PMC4910916.
22. Murphy EJ, Booth JC, Davrazou F, Port AM, Jones DN. Interactions of Anopheles gambiae odorant-binding proteins with a human-derived repellent: implications for the mode of action of n,n-diethyl-3-methylbenzamide (DEET). *J Biol Chem.* 2013 Feb 8;288(6):4475-85. doi: 10.1074/jbc.M112.436386. Epub 2012 Dec 23. PMID:

23261834; PMCID: PMC3567696.

23. Rafique B, Khalid AM, Akhtar K, Jabbar A. Interaction of anticancer drug methotrexate with DNA analyzed by electrochemical and spectroscopic methods. *Biosens Bioelectron.* 2013 Jun 15;44:21-6. doi: 10.1016/j.bios.2012.12.028. Epub 2012 Dec 27. PMID: 23384765.

24. Chen J, Zhang Y, Zhang Y, Zhao L, Chen L, Chai Y, et al. Host-guest inclusion for enhancing anticancer activity of pemetrexed against lung carcinoma and decreasing cytotoxicity to normal cells. *Chin Chem Lett.* 2021;32(10):3034-38. doi: 10.1016/j.ccllet.2021.03.079.

25. Bae JY, Lee GE, Park H, Cho J, Kim J, Lee J, et al. Antiviral Efficacy of Pralatrexate against SARS-CoV-2. *Biomol Ther (Seoul).* 2021 May 1;29(3):268-272. doi: 10.4062/biomolther.2021.032. PMID: 33731494; PMCID: PMC8094065.

26. Abdellatif KR, Abdelall EK, Abdelgawad MA, Ahmed RR, Bakr RB. Synthesis and anticancer activity of some new pyrazolo[3,4-d]pyrimidin-4-one derivatives. *Molecules.* 2014 Mar 18;19(3):3297-309. doi: 10.3390/molecules19033297. PMID: 24647032; PMCID: PMC6270843.

27. Alharthy RD. Design and Synthesis of Novel Pyrazolo[3,4-d]Pyrimidines: In Vitro Cytotoxic Evaluation and Free Radical Scavenging Activity Studies. *Pharm Chem J.* 2020;54:273-278. doi: 10.1007/s11094-020-02190-2.

28. Hassan A, Mady M, Awad H, Hafez T. Synthesis and antitumor activity of some new pyrazolo[1,5-a]pyrimidines. *Chin Chem Lett.* 2017;28(2):388-93. doi: 10.1016/j.ccllet.2016.10.022.

29. Dorababu A. Pyrazolopyrimidines as attractive pharmacophores in efficient drug design: A recent update. *Arch Pharm (Weinheim).* 2022 Oct;355(10):e2200154. doi: 10.1002/

ardp.202200154. Epub 2022 Jun 13. PMID: 35698212.

30. Elgemeie GH, Azzam RA, Zaghary WA, Khedr MA, Elsherif GE. Medicinal Chemistry of Pyrazolopyrimidine Scaffolds Substituted with Different Heterocyclic Nuclei. *Curr Pharm Des.* 2022;28(41):3374-3403. doi: 10.2174/1381612829666221102162000. PMID: 36330628.

31. Robins RK. Potential Purine Antagonists. I. Synthesis of Some 4,6-Substituted Pyrazolo [3,4-d] pyrimidines I. *J Am Chem Soc.* 1956;78(4):784-790.

32. Daina A, Michielin O, Zoete V. SwissADME: a free web tool to evaluate pharmacokinetics, drug-likeness and medicinal chemistry friendliness of small molecules. *Sci Rep.* 2017 Mar 3;7:42717. doi: 10.1038/srep42717. PMID: 28256516; PMCID: PMC5335600.

33. Veber DF, Johnson SR, Cheng HY, Smith BR, Ward KW, Kopple KD. Molecular properties that influence the oral bioavailability of drug candidates. *J Med Chem.* 2002 Jun 6;45(12):2615-23. doi: 10.1021/jm020017n. PMID: 12036371.

34. Muegge I. Selection criteria for drug-like compounds. *Med Res Rev.* 2003 May;23(3):302-21. doi: 10.1002/med.10041. PMID: 12647312.

35. Attique SA, Hassan M, Usman M, Atif RM, Mahboob S, Al-Ghanim KA, et al. A Molecular Docking Approach to Evaluate the Pharmacological Properties of Natural and Synthetic Treatment Candidates for Use against Hypertension. *Int J Environ Res Public Health.* 2019 Mar 14;16(6):923. doi: 10.3390/ijerph16060923. PMID: 30875817; PMCID: PMC6466102.

36. Unnisa A, Abouzied AS, Baratam A, Lakshmi KC, Hussain T, Kunduru RD, et al. Design, synthesis, characterization, computational study and in-vitro antioxidant and anti-inflammatory activities of few novel 6-aryl substituted pyrimidine azo dyes. *Arab J Chem.* 2020;13(12):8638-8649.

